

Coupled surface plasmon resonance on rotated sinusoidal gratings at different azimuthal orientations

M. Csete*, A. Szalai, E. Tóth, A. Somogyi, J. Balázs and G. Szabó

Department of Optics and Quantum Electronics, University of Szeged,
6720 Szeged, Dóm tér 9, Hungary

* mcsete@physx.u-szeged.hu

ABSTRACT

Dispersion characteristics of rotated wavelength-scaled dielectric-metal interfacial gratings with two different multilayer compositions corresponding to the same modulation amplitude was investigated. It was shown that double reflectance minima appear inside a finite spectral region in between two different azimuthal orientations: at 0° azimuthal angle (P-orientation) and at $\sim 30^\circ$ azimuthal angle (C-orientation). The modes propagating in the valleys are short-range in P-orientation, while the coupled modes confined at valley-edges exhibit long-range SPP features in C-orientation. Their E-field distribution and large propagation length is promising in bio-sensing applications.

Keywords: surface plasmon resonance, grating, coupling, short-range SPP, long-range SPP, biosensing

1 INTRODUCTION

Wavelength-scaled, moreover sub-wavelength gratings are important in tailoring the dispersion characteristics of SPPs propagating on metal-dielectric multilayers [1]. A small fraction of grating-related investigations was devoted to the special configuration nominated as conical mounting, namely when the plane of incidence is rotated with respect to the grating wave vector [2]. It has been shown, that the optical response in conical mounting is rotation sensitive, which makes biosensing challenging in this configuration [3]. An interesting configuration is, when a surface mode with the same mode index, but with different propagation directions can be coupled on gratings [4].

In our previous studies we have shown that the rotated grating coupling surface plasmon resonance (RGC-SPR) phenomenon can result in double peaked reflectance curves, when the SPP resonance is interrogated at constant wavelength [5, 6]. The advantage of the RGC-SPR phenomenon is that additional secondary reflectance minima appear at smaller polar angles, which possess smaller FWHM, making possible to realize bio-sensing with enhanced sensitivity.

Numerical investigation of the rotated grating coupling phenomenon was performed on multilayers comprising 416 nm periodic sinusoidal polymer gratings with 35 nm

modulation amplitude aligned on a bimetal film made of 7 nm gold and 38 nm silver layers.

The thin-uncovered chip consisted of 0 nm and 35 nm polymer layers in the valleys and at the hills, while the polymer layers were 15 nm and 50 nm in case of the thick-covered chip. The polar and azimuthal orientations were varied during 532 nm wavelength p-polarized light illumination.

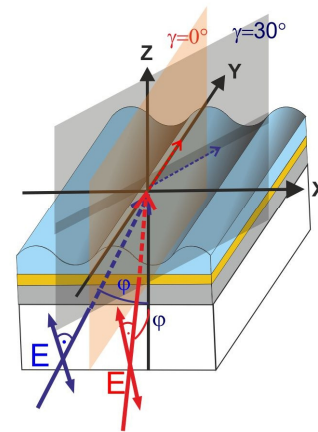


Figure 1: Schematic drawing about the polar and azimuthal angle tuning during the inspection of grating-coupling phenomenon in conical mounting.

2 RESULTS

In P-orientation of the thin-uncovered chip the dispersion curve indicates only a weak coupling (Fig. 2). At 532 nm the first minimum is observable at $\phi=49.0^\circ$, while the second minimum appears at $\phi=52.8^\circ$.

At the first minimum the E-field is dominantly concentrated at the glass side with $p/2$ periodicity, while there is a weaker E-field on the polymer side as well, resulting in local enhancement at both hills, however the enhancement is slightly stronger on the right side of the valleys (Fig 2aa, ab). At the second minimum enhanced E-field appears at both the glass and polymer side with p periodicity, and the intensity of the E-field is commensurate on the hills at the polymer side and below the valleys at the glass side (Fig 2ba, bb).

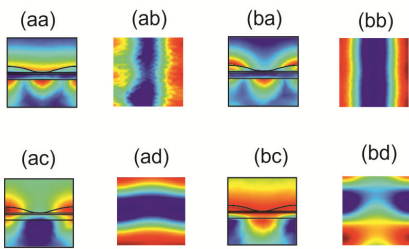
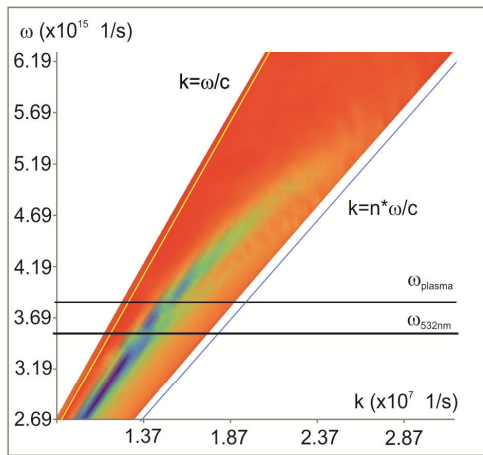


Figure 2: Dispersion characteristics of the reflectance on the thin-uncovered sinusoidal grating (0 nm and 35 nm PC in valleys and at hills), in P-orientation: $\gamma=0^\circ$. The near-field pictures show the vertical and horizontal cross-sections about the normalized \mathbf{E} -field / E_y component: (aa, ab / ac, ad) first minimum at $\varphi=49.0^\circ$, $\gamma=0.0^\circ$, and (ba, bb / 1bc, bd) second minimum at $\varphi=52.8^\circ$, $\gamma=0.0^\circ$.

In P-orientation distribution of the longitudinal \mathbf{E} -field component is symmetrical both vertically and horizontally at the first minimum, revealing that short-range plasmon is coupled (Fig 2ac, ad), while at the second minimum the \mathbf{E} -field is antisymmetric vertically at the hills, indicating that the coupled mode possesses long-range SPP characteristic (Fig. 2bc, bd). However, the location of this long-range SPP is not advantageous, taking into account that the bio-molecules prefer to attach into the valleys.

In C-orientation of the thin-uncovered chip the dispersion curve possesses a more well-defined coupling, and the strong-coupling between modes results in secondary and primary resonance minima (Fig. 3). At 532 nm the secondary and primary minima appear at $\varphi=48.6^\circ$ and $\varphi=54.0^\circ$ incidence angles at $\gamma=33.6^\circ$ azimuthal orientation. At both minima the \mathbf{E} -field is concentrated with p periodicity at the polymer-side, and are confined asymmetrically at the right edge of the valleys (Fig 3aa, ab and Fig 3ba, bb). The distributions of the longitudinal \mathbf{E} -field component is asymmetric both vertically and horizontally proving the co-existence of a standard and unique long-range grating coupled modes both at the secondary and primary minimum (Fig 3ac, ad, Fig 3bc, bd).

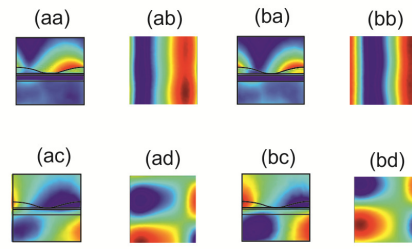
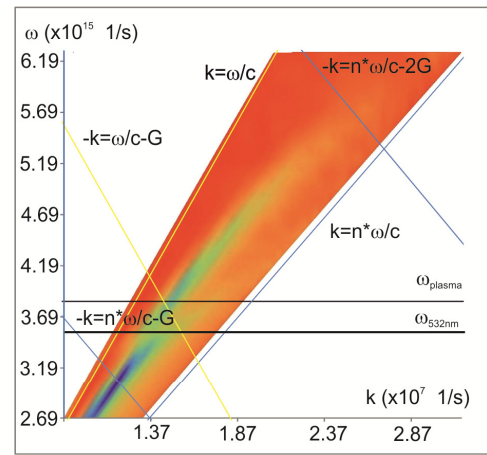


Figure 3: Dispersion characteristics of the reflectance on the thin-uncovered sinusoidal grating (0 nm and 35 nm PC in valleys and at hills), in C-orientation: $\gamma=33.6^\circ$. The near-field pictures show the vertical and horizontal cross-sections about the normalized \mathbf{E} -field / E_y component: (aa, ab / ac, ad) secondary minimum at $\varphi=48.6^\circ$, $\gamma=33.6^\circ$, and (ba, bb / 1bc, bd) primary minimum at $\varphi=54.0^\circ$, $\gamma=33.6^\circ$.

The dispersion characteristic exhibits more pronounced coupling phenomena and the near-field is slightly different in case of thicker polymer cover-layer (Fig. 4 and 5).

In P-orientation of the thick-covered chip the dispersion curve indicates a well defined coupling (Fig. 4). At 532 nm the first minimum is observable at $\varphi=52.0^\circ$ and the second minimum appears at $\varphi=61.0^\circ$. At the first minimum the \mathbf{E} -field is dominantly concentrated at the glass side with $p/2$ periodicity, while there is a weaker \mathbf{E} -field on the polymer side as well, resulting in local and symmetrical enhancement at both edges of the valleys (Fig 4aa, ab). At the second minimum enhanced \mathbf{E} -field appears at both the glass and polymer side with p periodicity, however the \mathbf{E} -field is most strongly concentrated on the hills at the polymer side and it is only weakly enhanced below the valleys at the glass side (Fig 4ba, bb). The distribution is completely symmetrical both vertically and horizontally in the longitudinal \mathbf{E} -field component both at the first and second minimum revealing that short-range plasmons are coupled at both minima in P-orientation of the thick-covered chip (Fig 4ac, ad and Fig. 4bc, bd).

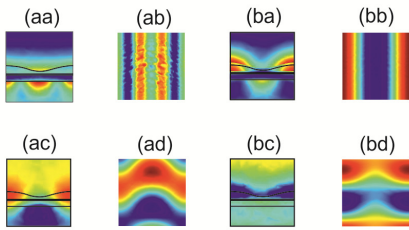
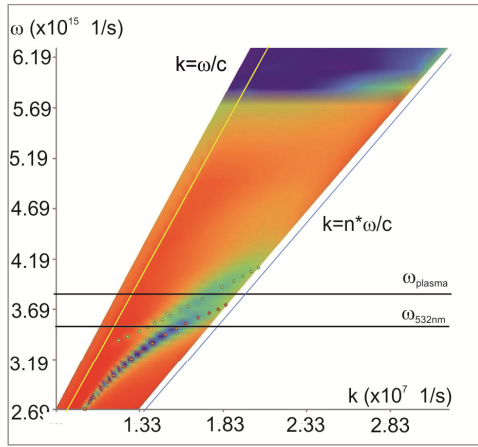


Figure 4: Dispersion characteristics of the reflectance on the thick-covered sinusoidal grating (15 nm and 50 nm PC in valleys and at hills), in P-orientation: $\gamma=0.0^\circ$. The near-field pictures show the vertical and horizontal cross-sections about the normalized **E**-field / E_y component: (aa, ab / ac, ad) first minimum at $\phi=52.0^\circ$, $\gamma=0.0^\circ$, and (ba, bb / 1bc, bd) second minimum at $\phi=61.0^\circ$, $\gamma=0.0^\circ$.

In C-orientation of the thick-covered chip the strong-coupling between modes results in well defined secondary and primary resonance minima on the reflectance (Fig. 5). At 532 nm the secondary and primary minima appear at $\phi=57.0^\circ$ and $\phi=63.0^\circ$ incidence angles at $\gamma=30.0^\circ$ azimuthal orientation. At both minima the **E**-field is concentrated with p periodicity at the polymer-side, and the field maxima are confined asymmetrically at the right edge of the valleys (Fig 5aa, ab, Fig 5ba, bb). However, there is a well defined difference between the distributions of the longitudinal **E**-field component, which is vertically asymmetric and symmetric proving the existence of a standard long- and short-range coupled modes at the secondary and primary minimum, respectively (Fig 5ac, ad and Fig 5bc, bd). This difference between the minima indicates that the long-range nature of the coupled mode is preserved at the secondary minimum also in case of thicker polymer cover layers. In addition to this the coupled modes exhibit antisymmetry in the longitudinal **E**-field component horizontally with respect to the right edge of the valley, which proves the co-existence of unique long-range modes (Fig 5ad and Fig 5bd). The antisymmetry of the longitudinal **E**-field indicates that the modes' attenuation is minimized, which is advantageous in several applications [7].

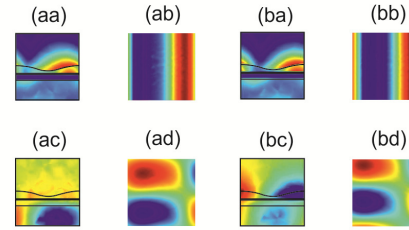
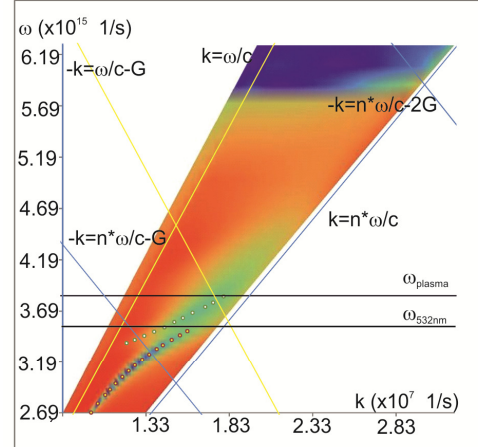


Figure 5: Dispersion characteristics of the reflectance on the thick-covered sinusoidal grating (15 nm and 50 nm PC in valleys and at hills), in C-orientation: $\gamma=30.0^\circ$. The near-field pictures show the vertical and horizontal cross-sections about the normalized **E**-field / E_y component: (aa, ab / ac, ad) secondary minimum at $\phi=57.0^\circ$, $\gamma=30.0^\circ$, and (ba, bb / 1bc, bd) primary minimum at $\phi=63.0^\circ$, $\gamma=30.0^\circ$.

On the inspected thin-uncovered and thick-covered gratings the strongest coupling appears at the Brillouin zone boundary independently of azimuthal orientation. The coupling appears in very similar region in case of the same modulation amplitude, however the strength of coupling increases with the polymer layer thickness in the valley and at the hills. The coupling occurs in the region of bands corresponding to photonic and plamonic modes, which are grating coupled in -1 order on the sub-wavelength grating.

The modes appearing at the first and second minimum in P-orientation corresponds to the eigenmodes of the multilayer, which propagate along the valleys and hills. Although, the normalized **E**-field is very similar at the secondary and primary minima in C-orientation, both the field distribution at and the origin of the secondary minimum is unique. The secondary minimum originates from a scattering process on the wavelength-scaled grating, which is capable of coupling into a mode propagating along the valley and having a mode index similar to that one of the eigenmodes, which is observable at the first minimum in P-orientation. However, due to its antisymmetric longitudinal **E**-field component, this mode does not suffer attenuation, has long propagation distance, accordingly it can be considered as a long-range SPP.

The secondary minimum in C-orientation is proposed for biosensing applications, since the biomolecules prefer to attach into the valleys, where the rotated grating coupling phenomenon results in E-field enhancement with unique distribution promoting large interaction cross-sections between the grating-coupled modes and the molecules to be detected.

ACKNOWLEDGEMENT

The research was supported by National Research, Development and Innovation Office-NKFIH through project “Optimized nanoplasmonics” K116362. Mária Csete acknowledges that the project was supported by the János Bolyai Research Scholarship of the Hungarian Academy of Sciences. Gábor Szabó acknowledges the support of Hungarian Academy of Sciences.

REFERENCES

- [1] W. L. Barnes, T. W. Preist, S. C. Kitson, and J. R. Sambles, “Physical origin of photonic energy gaps in the propagation of surface plasmons on gratings,” *Phys. Rev. B* 54(9), 6227–6244, 1996.
- [2] M. Kretschmann, T. A. Leskova, A. A. Maradudin, “Conical propagation of a surface polariton across a grating”, *Optics Communications* 215(4-6), 205-223, 2003.
- [3] D. Kim, “Effect of the azimuthal orientation on the performance of grating-coupled surface-plasmon resonance biosensors,” *Appl. Opt.* 44, 3218-3223, 2005.
- [4] F. Romanato, L. K. Hong, H. K. Kang, C. C. Wong, Z. Yun, and W. Knoll, “Azimuthal dispersion and energy mode condensation of grating-coupled surface plasmon polaritons” *Phys. Rev. B* 77, 245435, 2008.
- [5] M. Csete, A. Köházi-Kis, V. Megyesi, K. Osvay, Z. Bor, M. Pietralla, O. Marti, “Coupled Surface Plasmon Resonance on Bimetallic Films Covered by Sub-micrometer Polymer Gratings”, *Organic Electronics* Vol. 8 No. 2-3, 148-160, 2007.
- [6] A. Szalai, G. Szekeres, J. Balázs, A. Somogyi, M. Csete, “Rotated grating coupled surface plasmon resonance on wavelength-scaled shallow rectangular gratings”, in *Proc. SPIE* 8809, *Plasmonics: Metallic Nanostructures and Their Optical Properties XI*, 88092U (September 11, 2013); doi:10.1117/12.2024527.
- [7] S. I. Bozhevolnyi, T. Sondegaard: “General properties of slow-plasmon resonant nanostructures: nano-antennas and resonators”, *Optics Express* 15/16, 10869-10877, 2007.